Published in final edited form as:
J Physiol Paris. 2009 ; 103(3-5): 149–158. doi:10.1016/j.jphysparis.2009.08.001.

Comparison of Human and Humanoid Robot Control of Upright Stance

Robert J. Peterka, Ph.D
Biomedical Engineering Division, Oregon Health & Science University, OHSU West Campus, Mail Code NSI, 505 NW 185th Avenue, Beaverton, Oregon 97006, USA

Abstract

There is considerable recent interest in developing humanoid robots. An important substrate for many motor actions in both humans and biped robots is the ability to maintain a statically or dynamically stable posture. Given the success of the human design, one would expect there are lessons to be learned in formulating a postural control mechanism for robots. In this study we limit ourselves to considering the problem of maintaining upright stance. Human stance control is compared to a suggested method for robot stance control called zero moment point (ZMP) compensation. Results from experimental and modeling studies suggest there are two important subsystems that account for the low- and mid-frequency (DC to ~1 Hz) dynamic characteristics of human stance control. These subsystems are 1) a “sensory integration” mechanism whereby orientation information from multiple sensory systems encoding body kinematics (i.e. position, velocity) is flexibly combined to provide an overall estimate of body orientation while allowing adjustments (sensory re-weighting) that compensate for changing environmental conditions, and 2) an “effort control” mechanism that uses kinetic-related (i.e., force-related) sensory information to reduce the mean deviation of body orientation from upright. Functionally, ZMP compensation is directly analogous to how humans appear to use kinetic feedback to modify the main sensory integration feedback loop controlling body orientation. However, a flexible sensory integration mechanism is missing from robot control leaving the robot vulnerable to instability in conditions were humans are able to maintain stance. We suggest the addition of a simple form of sensory integration to improve robot stance control. We also investigate how the biological constraint of feedback time delay influences the human stance control design. The human system may serve as a guide for improved robot control, but should not be directly copied because the constraints on robot and human control are different.

Keywords

Robot; human; stance control; zero moment point; ZMP; sensory integration

Corresponding Author: Robert J. Peterka, Ph.D., Biomedical Engineering Division, Oregon Health & Science University, OHSU West Campus, Mail Code NSI, 505 NW 185th Avenue, Beaverton, Oregon 97006, USA, peterkar@ohsu.edu, Phone: +1-503-418-2616, Fax: +1-503-418-2701.

1. Introduction

The human stance control system can be viewed as a conglomeration of subsystems that are configured to achieve the goal of maintaining stance and compensating for internal and external disturbances while overcoming the constraints imposed by biology (Horak and Macpherson, 1996). The ability to maintain upright stance confers survivability advantages by allowing humans to operate in a variety of environments that sometimes limit the availability or accuracy of sensory orientation cues (e.g. absence of vision, stance on compliant surfaces, altered inertial environments), under conditions that alter the mechanics of the system (e.g. changing loads, different body postures, altered gravity), and in conditions were unexpected external or internal perturbations are applied (e.g. external forces, moving surface, moving visual surround, sensory dysfunction).

In contrast to human stance control, robot stance control is at an early stage of evolution. The need for some form of stance control system has been recognized during the recent rapid development of humanoid robots (see Mahboobin et al., 2008). However, the design of most robot balance systems has not taken advantage of existing knowledge of human stance control systems. A possible reason for this is that engineers focused on the obviously important interaction that occurs at the interface between the robot's feet and the ground. This interaction can be measured using force sensors in the feet to calculate the center-of-pressure (COP) position which represents the location of the equivalent point of application of net ground reaction force. In static conditions, the projection of the body center-of-mass (COM) position onto the ground corresponds to the COP location. This provides some intuitive notion that COP location includes information about COM location, and that stability is ensured if the COM and COP location remains within the base-of-support (i.e. within or between the outline of the feet).

The COP corresponds to what is termed the zero moment point (ZMP) under conditions where the system is statically or dynamically balanced (Vukobratovic and Borovac, 2004). Engineers have utilized the ability to measure and to calculate the ZMP to develop control methods known as ZMP compensation for robot stance control, disturbance compensation, and motion control under dynamically balanced conditions (Caballero et al., 2006; Prahlad et al., 2008).

In a freestanding human or robot in both static and dynamic situations, the COP is proportional (to a good approximation) to the corrective torque, T_c, exerted about the ankle joint by the stance control system (van der Kooij et al., 2005). Specifically

$$x_{COP}=\frac{-T_c}{mg} \tag{1}$$

where m is the body mass (not including the feet) and g is acceleration due to gravity.

Additionally, for a simplified mechanical system where the body is represented by a single-link inverted pendulum, the COP displacement (x_{COP}) is proportional (again to a good approximation) to a linear combination of COM displacement (x_{COM}) and COM acceleration ($\ddot{x}_{COM}$) (Winter et al., 1998)

$$x_{COP}=x_{COM}-\frac{J}{mgh}\ddot{x}_{COM} \tag{2}$$

where J is body moment of inertia about the ankle joint, m is body mass, and h is height of the COM above the ankle joint. From this equation, one can see that any deviation of x_{COP} from

x_{COM} will produce an acceleration of the body. Therefore, a control system that can keep x_{COM} and x_{COP} closely aligned will limit the acceleration of the COM and therefore will provide for stable stance.

Because of the relationship between COP and corrective torque, one can say that a control system making use of COP information is making use of kinetic (i.e. force-related) information for stance control. In the ZMP compensation method described by Prahlad et al. 2008 and similarly by Cabellero et al., 2006 (Caballero et al., 2006), this kinetic information provides a setpoint for a control system that regulates the ankle joint angle. This ankle joint control system can be thought of as using kinematic information (i.e. ankle joint angular position and velocity information) to regulate ankle joint angle. Therefore, the overall ZMP compensation scheme combines kinetic and kinematic information for stance control.

There is some general correspondence between ZMP compensation and human stance control regarding the combined use of kinetic and kinematic orientation information. Specifically, there is evidence that human subjects make use of force-related information derived from somatosensors in the feet (Magnusson et al., 1990; Maurer et al., 2001) as well as kinematic information derived from ankle proprioceptors for stance control (Kavounoudias et al., 1999). However, it has long been known that humans make use of orientation information from other sensory systems such as graviception provided by the vestibular system and vision (Day et al., 1997; Hlavacka and Njiokiktjien, 1985; Lee and Lishman, 1975; Nashner and Berthoz, 1978). One purpose of this paper is to make an explicit comparison between a robotic stance control system using ZMP compensation and the human balance control system, and to show how the human system has been extended to incorporate orientation information from other sensory systems.

Are there any limitations to the use of ZMP compensation for robot stance control? This paper will demonstrate that there are limitations, but will illustrate how some of these limitations can be overcome by incorporating graviceptive information in a manner related to the human control system. One might argue, then, that it would be better to build a robotic stance control system that closely mimics human control, as best we currently understand it (Mergner, 2007; Mergner et al., 2006; Tahboub and Mergner, 2007). However, the human system was designed by evolutionary forces that presumably accounted for various biological constraints. These constraints include (1) time delays associated with both the transmission of sensory and motor signals and with the neural processing required to interpret distributed raw sensory signals and to integrate (fuse) orientation information from multiple sensor systems, (2) the complex properties of muscles including muscle activation and contraction dynamics, (3) the dynamics of force generation via muscle/tendon systems, (4) the problem of transmitting sufficient force through compliant tendons, (5) the requirement to generate coordinated activation of multiple muscles, (6) the noise or variability in sensory and motor systems that limits the accuracy of sensory orientation estimates and reduces the ability to deliver precise motor responses. These biological constraints generally are not the same as those involved in robot design. Therefore one would expect that a robotic control system that simply mimics human control would likely be sub-optimal. This point is illustrated by demonstrating how a biological constraint (feedback time delay), which would not necessarily be a constraint in a robot design, is likely to have influenced the design of the human stance control system.

2. Methods

All results are derived from mathematical simulations of model control systems that represent the mechanisms that regulate the upright stance of robots or humans. The body mechanics are those of a single-link inverted pendulum represented by a linearized differential equation

$$J\frac{d^2BS\ (t)}{dt^2}=mghBS\ (t)+T_c \tag{3}$$

where *BS* is the body-in-space sway angle with respect to earth-vertical. Other variables were previously defined for Equations 1 and 2. Values of *J*, *m*, and *h* are given in Table 1 along with other model parameters defined later. COP displacement was calculated using Equation 1.

Equation 3 can also be represented as an algebraic equation relating the output (*BS*) to the input (T_c) by taking the Laplace transform of Equation 3

$$\frac{BS\ (s)}{T_c\ (s)}=\frac{1}{Js^2-mgh} \tag{4}$$

where *s* is the Laplace variable.

With a Laplace domain representation of body mechanics as well as other components of the stance control system, it is easy to write an equation that relates various potential input disturbances (stimuli), such as tilt of the support surface or an external force applied to the body, to output responses which we will take to be either *BS*, COM displacement, or COP displacement. By substituting $s=j\cdot 2\pi f$ into the overall Laplace domain equation of the control system, where *j* is the imaginary number $\sqrt{-1}$ and *f* is frequency (in Hz), one can calculate the frequency response function (FRF) representing how the dynamic characteristics of the system transform a sinusoidal input stimulus to an output response. The FRF can be expressed as gain and phase curves that vary as a function of frequency. The gain value of the FRF at any particular frequency gives the ratio of response magnitude to stimulus magnitude, and the phase (in degrees) represents the relative timing between the stimulus and response. The dynamic properties of the overall system are characterized by the particular pattern of gain and phase changes with frequency.

The dynamic characteristics of a ZMP robot control system and of models that have previously been shown to accurately represent the dynamic characteristics of human stance control (Cenciarini and Peterka, 2006; Peterka, 2002, 2003) will be illustrated by showing their FRFs and by showing time domain responses of these systems to step stimuli. The time domain responses were generated using Matlab version 7.5 and Simulink version 7.0 (The MathWorks Inc., Natick, MA, USA).

The disturbances investigated included 1) application of a external force which applies a torque (T_{ext}) to the body of the simulated human subject or robot, 2) rotations of the support surface upon which the simulated human subject or robot stands, and 3) sway-referencing of the support surface (Nashner, 1982). Sway-referencing is a particularly challenging disturbance whereby the support surface is rotated in equal proportion to the body sway angle with respect to earth vertical. This results in a fixed ankle joint angle such that an ankle joint angle sensor no longer encodes any useful information about the body orientation in space. However in a sway-referenced condition, a human or robot can still exert a corrective torque about the ankle joint to maintain balance if the stance-control system can make use of alternative sensory information that encodes body sway relative to earth vertical.

3. Results

3.1 Model of Robot Stance Control

A block-diagram model of ZMP compensation as it applies to robot stance control is shown in Fig. 1A. The block-diagram shows two control loops. Loop 1 uses negative feedback control to regulate the ankle-joint angle. By analogy to human stance control (Fig. 1B), this loop corresponds to the use of ankle proprioception to stabilize stance. The inherently unstable inverted-pendulum body is stabilized by a "controller" that generates a corrective torque, T_c, in proportion to a combination of body sway angular position and velocity. The gain constants K_P and K_D in the controller determine the amount of position-related and velocity-related torque, respectively. The value of K_P must be larger than *mgh* in order to counteract the destabilizing torque due to gravity. The other constraint on K_P and K_D is the need to limit their magnitude so that the torque generated by postural corrections would not lift the feet off the ground and the ZMP does not move to the edge of the base-of-support. Within these constraints, the particular values of K_P and K_D are fairly arbitrary and could be selected based on other design criteria (torque limitations, energy considerations, specific stability criteria).

Loop 2 implements ZMP compensation. In a real robot, force sensors in the robot's feet would be used to calculate the COP location. In the model, Equation 1 is implemented to calculate COP based on T_c. The COP signal is scaled by the gain factor K_{COP}, low-pass filtered (time constant τ_{COP}), and subtracted from the signal in Loop 1 representing the difference between the support surface (*SS*) tilt position and *BS*. This ZMP control scheme is directly related to the one discussed in Caballero et al., 2006, but differs from that of Prahlad et al., 2008. Prahlad used the force sensor information to detect a ZMP that was outside of a specified threshold and then used the ZMP value to calculate a new ankle-joint reference offset command angle for the ankle-joint control loop (Loop 1). This is a non-linear control scheme that is not represented by the continuous control model in Fig. 1A. Thus, there are different ways to make use of ZMP information for robot stance compensation. This paper focuses on the linear control scheme utilized by Caballero et al., 2006 because this scheme appears to resemble most a mechanism utilized by humans.

Note that although the filtered COP signal is subtracted from the *SS-BS* signal, Loop 2 effectively provides positive feedback. For example, if the robot is initially leaning forward, *SS-BS* will be negative and T_c will have a negative value proportional to the forward body lean. A negative value of T_c produces a positive COP displacement (Equation 1). When the filtered positive COP value is subtracted from *SS-BS*, the controller input signal will become more negative and a more negative T_c value will be generated. The larger negative T_c value will overcome the torque due to gravity, and will thus move the body back toward an upright position. The positive feedback nature of Loop 2 is appreciated by noting that Loop 2 operating in isolation will always generate at time $t+\Delta t$ a larger magnitude value of T_c with the same sign than was present at time *t*.

Positive feedback loops are typically associated with instability. Loop 2 alone is unstable, but when operated in conjunction with Loop 1 the overall system can be stable for appropriate values of Loop 2 parameters K_{COP} and τ_{COP}. For stable operation as a positive feedback loop, a low-pass filter or mathematical integrator is required in Loop 2. It can be show that without the low-pass filter (i.e., τ_{COP} set to zero) the value of K_{COP} would have to have a negative value between -1/*h* and zero. The negative valued K_{COP} required for stability when $\tau_{COP} = 0$ means that the COP feedback loop would be providing negative feedback. Although the system could be stable with negative COP feedback and with $\tau_{COP} = 0$ the overall system would not provide the desired compensation for disturbances.

A wide range of K_{COP} and τ_{COP} parameters are compatible with stability. The particular parameters shown in Table 1 were selected based on simulation results such as those shown in Figs. 2B and 3B. The goal was to find parameters that gave non-resonant responses that quickly reached steady-state conditions while generating peak COP amplitudes that were well within the base-of-support in a robot with human size feet.

3.1.1 Robot response to external force perturbations—The FRFs for external torque, T_{ext}, perturbations applied by an external force acting at COM level are shown in Fig. 2A. The response is *BS* tilt. In addition to the human FRF discussed later, two sets of curves are shown for the robot. One set is for a robot with only Loop 1 control (i.e., without ZMP compensation) and the other with both Loop 1 and Loop 2 control (i.e., with ZMP compensation). The two gain curves are very similar. This might be interpreted as indicating that the addition of ZMP compensation had very little effect on responses to T_{ext}. However, the effect of ZMP compensation is clearly evident in the phase curves. The phase curve for control with ZMP compensation shows a phase lead approaching 180° at low frequencies while the low frequency phase is approximately 0° for Loop 1 control. A 180° phase shift represents a sign inversion indicating that the COM is moving opposite to the applied force, e.g. the body sways backward when a forward directed force is applied. Functionally, this control scheme can be thought of as using the torque due to gravity acting on the body to cancel the disturbance caused by T_{ext}.

The effect of ZMP compensation is more easily seen in the time domain step responses shown in Fig. 2B. Without ZMP compensation, a T_{ext} step change of +10 Nm produces a sustained forward (positive) *BS*, COM displacement, and COP displacement. The larger amplitude of COP displacement compared to COM displacement reflects the fact that the total corrective torque generated must compensate for T_{ext} in addition to body tilt. With ZMP compensation, the same +10 Nm T_{ext} initially causes a very slight transient forward displacement of *BS*, but then the ZMP compensation causes a transient corrective torque to be generated, as reflected by the transient positive COP displacement, that drives the body backward such that when steady state conditions are reached, the COP is only slightly forward of the ankle joint and the body is leaning backwards (negative *BS* and COM displacement). Effectively, the ZMP compensation loop is tightly regulating the final COP displacement to keep it located close to the ankle joint.

3.1.2 Robot response to surface tilt perturbations—The FRFs for support surface, *SS*, tilt perturbations are shown in Fig. 3A both with and without ZMP compensation (in addition there are two human FRFs). The robot gain and phase curves are quite different from one another. For the case without ZMP, the *BS*/*SS* gain curve has greater than unity values across much of the frequency range and approaches a value of $K_P/(K_P - mgh)$ at low frequencies. Gains greater than unity indicate that the body tilts further than the surface tilt. The addition of ZMP compensation greatly reduces the gain at lower frequencies. Lower gains are desirable in that they indicate that the body would remain closer to an upright orientation in response to surface tilts.

The time domain responses shown in Fig. 3B demonstrate the effect of ZMP compensation. Without ZMP, a 1° toe down tilt of the surface (positive sign) produces a steady state forward body tilt of about 1.6° for the model parameters used in the simulations. With ZMP, *BS* quickly returns to a value close to zero following a step change in surface tilt. The COM displacement is proportional to *BS*. Both with and without ZMP, the COP displacement shows a biphasic transient. The first phase has negative sign and is associated with the generation of a positive corrective torque that initially moves the body forward toward alignment with the tilted surface. The second phase has positive sign and is associated with the generation of a negative corrective torque. Without ZMP compensation, the second phase transient arrests the forward body motion and then a positive COP value is maintained to hold the body in a forward leaning position. With ZMP compensation, the larger magnitude COP transient acts to arrest forward body motion and then to return the body to an orientation that is very close to upright.

Although the model in Fig. 1A applies to stance control, one could anticipate that the ZMP control scheme could be incorporated into a dynamically balanced walking robot to provide improved control of body orientation (where dynamic balance means that the COM and COP always remain within the base-of-support). If the ZMP control scheme were utilized in a dynamically balanced walking robot that was moving up or down a sloped ramp, the ZMP control would cause the robot to appropriately lean forward or backward, respectively, to compensate for the surface slope while it executed the motions necessary for walking. This was demonstrated by Prahlad et al., 2008 although their ZMP control scheme was slightly different than the one shown in Fig. 1A. Note, however, that balance control schemes that apply to stance control and dynamically balanced walking robots would not necessarily be applicable for other forms of walking control. Specifically, "dynamic walking" robots (Collins et al., 2005), that appear to closely resemble human walking, would not necessarily satisfy the criterion that COP remain within the base-of-support and thus could not be controlled using the regulation schemes shown in Fig. 1.

One might assume that the time course of compensation for external disturbances would be quite slow and perhaps not functionally useful given the fairly long time constant (4.5 s for simulations in Fig. 2B and 3B) of the low-pass filter in the COP feedback loop. However, the compensation time course depends on the dynamic characteristics of the entire system. As is typical in feedback control systems, the overall system responsiveness can be faster than individual components within the system. The responses to disturbances shown Figs. 2B and 3B have a time constant of about 1 s and thus are considerably faster than the COP feedback loop itself.

3.2 Model of Human Stance Control

A simplified model of human stance control is shown in Fig. 1B. This model was developed to account for experimental FRFs calculated from body sway responses to wide-bandwidth pseudorandom perturbations that included tilts of the support surface and visual surround (Peterka, 2002,2003). The model presented here is simplified in that it only includes torque generation via an active, neurally mediated mechanism and does not include a mechanism for passive torque generation due to the mechanical properties of joints, muscles, and tendons. Our experimental results showed that passive mechanisms contributed only about 15% of the total corrective torque, although there is controversy about the relative contribution of passive mechanisms (Casadio et al., 2005;Loram and Lakie, 2002;Morasso and Sanguineti, 2002). Our original model (Peterka, 2002) included a PID (proportional, integral, derivative components) neural controller. The PID controller was not able to account for the FRF data below about 0.05 Hz. This motivated a later version of the model that utilized a torque feedback mechanism that was better able to account for lower frequency experimental gain and phase data (Cenciarini and Peterka, 2006;Peterka, 2003).

A comparison of the human stance control model (Fig. 1B) with the robot model (Fig. 1A) shows some structural similarities. The human model includes a feedback loop that uses kinematic ankle proprioception to generate corrective torque in relation to ankle joint motion. This loop is labeled Loop 1 since it corresponds exactly to the ankle joint feedback loop in the robot model. The model also includes a torque feedback loop that is labeled Loop 2 since it corresponds to the COP feedback in the robot model. Remember that the robot calculates COP (with sign inversion and 1/*mg* scaling) and subtracts a low-pass filtered version of this signal from the ankle joint angle signal. The human model feeds back a low-pass filtered version of T_c and adds it to the sensory error signal. Therefore, the functional correspondence of Loop 2 is identical in the human and robot models, and both provide positive feedback. The only difference is that the gain factor in the low-pass filter of the human model, K_{torq}, has different units than the corresponding gain factor in the robot model, K_{COP}.

There are also obvious structural differences between the human and robot models. First, the human model includes a significant time delay in its control loop that accounts for neural transmission times, sensory processing, and muscle activation delays. A time delay value of about 150 ms is required to account for experimental data (Maurer et al., 2006; Peterka, 2002). In contrast, the processing and transmission delays in a robot system are negligible and can be set to zero for modeling purposes. Second, the human model includes feedback from visual and vestibular systems that are not present in the robot. The experimental results revealed that FRF gains varied as a function of stimulus amplitude (Peterka, 2002). The model-based interpretation of these varying FRF gain curves is that humans are able to alter the source of sensory information used for stance control as a function of stimulus conditions. This "sensory re-weighting" is represented in the human model by weighting factors (W_{prop}, W_{vis}, W_{vest}) that represent the relative proportion of proprioceptive, visual, and vestibular sensory orientation information being used for stance control in a given test condition.

There are special cases where the human and robot models are the most similar. One case is a model representing a human with bilaterally absent vestibular function during eyes closed stance. This model is identical to the robot model except for the time delay term in the human model. A second case is a model representing a human perturbed by an external force during stance on a level surface while viewing an earth-fixed visual scene. In this case, proprioceptive, visual, and vestibular sensory systems are functionally equivalent in that they are all encoding body sway relative to earth-vertical. Therefore, the proprioceptive, visual, and vestibular feedback loops can be collapsed into one feedback loop. Again, this model is identical to the robot model except for the time delay term in the human model.

The FRFs and model simulations of human stance control discussed in sections 3.2.2 include these special cases where robot and human control are quite similar in order to illustrate how the presence or absence of a significant time delay affects control behavior.

3.2.1 Time delay constraint on human stance control—The presence of a time delay in a feedback control system can affect stability and therefore imposes a constraint on the design of the system. Figure 4 shows regions of stable operation for different selections of neural controller parameters K_P and K_D at several values of loop delay times. These stability regions were calculated for a model without the Loop 2 torque feedback. For a given time delay, the stability region is smaller when torque feedback is included and the region shrinks as the strength (gain) of the torque feedback increases. Independent of the time delay, the neural controller must generate torque of sufficient magnitude to resist the torque due to gravity. This constrains the value of K_P to be greater than mgh. The region of stable operation shrinks with increasing delay, and therefore further constrains the choice of neural controller settings. For human stance control, a time delay of about 150 ms is consistent with experimental data (Maurer et al., 2006;Peterka, 2002). The mean values of K_P and K_D parameters derived from model fits to experimental data are shown in Fig. 4 to lie inside the 250 ms stability region. This suggests that the human stance control system is conservatively designed to avoid instability due to time delays in feedback control.

In comparison to the human, the robot's stability benefits from having higher stiffness (K_P and K_D parameters) and a greater magnitude of torque feedback (robot K_{COP}/mg > human K_{torq}). However, with the robot parameters given in Table 1, the robot's stability would be very sensitive to any time delay in the system. Specifically, the robot would be unstable for any time delay greater than about 36 ms. This comparison illustrates the interaction among control parameters and shows the need to select robot control parameters based on the constraints of the robot system rather than simply replicating human control.

3.2.2 Human response to external force and surface tilt perturbations—Figures 2A,C and 3A,C shows FRFs and time domain step responses using the human control model (Fig. 1B). The FRFs for surface tilt stimuli (Fig. 3A) show the large effect of sensory reweighting on the gain curves from the two conditions with differing sensory weights. One condition represents a subject with absent vestibular function standing eyes closed (W_{prop}=1.0, W_{vest}=0, W_{vis}=0) (Peterka, 2002). The other condition represents a subject with normal sensory function standing eyes closed on a surface moving with a fairly large amplitude (W_{prop}=0.3, W_{vest}=0.7, W_{vis}=0). Although the FRF gain curves differ greatly in magnitude, the phase curves for the conditions are identical. Due to the loop time delay, these phase curves show much larger phase lags at higher frequencies than the corresponding robot phase curves. The step responses (Fig. 3C) show *BS*, COM displacement, and COP displacement responses for the two different sets of sensory weights.

The ability of humans to adjust sensory weights as a function of stimulus conditions confers an ability to resist perturbations by reducing the responsiveness of the system to the perturbing stimulus while still generating an adequate amount of corrective torque to resist the destabilizing torque due to gravity. This capability is not present in the robot control system. In addition, the fact that, for the human control system, 1) the phase characteristics as a function of stimulus conditions remain unchanged and 2) the overall shape of the gain curves remains unchanged (only the absolute gain changes) indicates that the fundamental dynamic properties of the system remain unchanged as a function of the changing surface tilt amplitude. That is, sensory re-weighting causes no change in the inherent stability of the system. A potential alternative strategy to sensory re-weighting for resisting the effects of a perturbation would be to increase the overall stiffness of the system by increasing the neural controller gains K_P and K_D. However, this strategy would require fairly large changes in controller gains to produce useful performance improvements. Such large changes would change the overall dynamic characteristics of the system, and could move the system close to or beyond a stability boundary.

In contrast to surface tilt responses, sensory re-weighting has no effect on the FRFs of body sway responses to T_{ext} (Fig. 2A). During stance on a level surface ankle proprioception, the vestibular system, and visual system all encode body tilt relative to earth vertical. Therefore, sensory re-weighting does not change the orientation signal available to the control system. The FRF gain values of the robot system are smaller than in the human system because the neural controller gain factors K_P and K_D were assumed to be twice as large in the robot system. The FRF phase values at lower frequencies for the human system are in between the phase values of the robot systems with ZMP and without ZMP compensation. The robot with ZMP compensation shows larger low frequency phase leads than the human because of the stronger influence of the ZMP compensation as compared to the torque feedback in the human system.

3.3 A case where robot stance control fails but human control succeeds

From the comparison of robot and human stance control models discussed above, it may seem that there are only minor differences between the dynamic characteristics of their control. However, the ability of the human system to make use of orientation information from multiple sensory sources and to use sensory re-weighting to rapidly change the source of sensory orientation cues as environmental conditions change provides a high level of robustness that is not present in the robot stance control system described in this paper.

A relevant example of this is the experimental manipulation referred to as “support surface sway-referencing”. Sway-referencing is accomplished experimentally by continuously monitoring the body sway angle with respect to earth-vertical, and then using this signal as the command input to a servo-system that controls the tilt angle of the support surface. The net effect is to lock the ankle joint angle to a fixed and unchanging value. The whole body can still sway and the subject can still exert torque about the ankle joint to control body sway.

Human subjects with normal sensory function are able to stand eyes closed on a sway-referenced surface because they are able to rapidly re-weight toward a reliance on vestibular orientation cues (Cenciarini and Peterka, 2006; Peterka and Loughlin, 2004). Consistent with this interpretation, subjects with bilaterally absent vestibular function fall with a pendular sway trajectory indicative of complete absence of control (Nashner et al., 1982).

The human control model (Fig. 1B) is consistent with these experimental results. Sway referencing effectively opens the proprioceptive feedback loop (Loop 1). That is, *SS* is commanded to be equal to *BS*. The input to ankle proprioception is *SS*-*BS*, which will be equal to zero with sway-referencing. Therefore, no corrective torque is generated by the proprioceptive feedback loop. However, if the vestibular sensory weight, W_{vest}, is set to unity value in the model, the vestibular signal will drive the generation of all of the corrective torque necessary to maintain eyes closed stance.

As mentioned previously, the robot model is directly analogous to the human model in the case of eyes closed stance and absent vestibular function. By the same arguments as given in the previous paragraph, the robot model is unstable in a sway-referenced condition. There are no parameter alterations to the ZMP compensation loop that can be made to provide stability since this loop provides positive feedback.

3.4 Improving robot stance control

An obvious improvement to the robot would be to make it more like the human system by adding a feedback loop that provides sensory information about body tilt relative to earth-vertical, i.e. add a vestibular system to the robot. However, with an additional negative feedback loop, the question is to what value should the sensory weights of these two loops be set, or should they be made adjustable depending on environmental conditions? There exists a non-linear model of balance control that incorporates a method of sensory re-weighting that mimics human performance (Maurer et al., 2006; Mergner, 2007) and its non-linear control scheme has been implemented in a bipedal robot (Mergner et al., 2006). But here we propose a simpler linear control model that has some level of robustness and at least improves upon the control scheme shown in Fig. 1A.

The proposed control system (Fig. 5A) simply adds a “body tilt” sensor (equivalent to the vestibular system in the human model) that feeds back a signal proportional to body orientation with respect to earth-vertical. The body tilt and ankle joint signals are multiplied by fixed and equal gain factors of value 0.5 to give equal weight to these signals (equivalent to W_{prop}=W_{vest}=0.5 in the human model). As in the previous robot models, the controller values K_P and K_D are kept at twice the values typical for humans.

The FRF and step responses to external torque perturbations are identical to those shown for the previous robot model with ZMP compensation (Fig. 2A,B) because the body tilt sensor and ankle joint sensor both signal body orientation with respect to earth-vertical under the conditions of this perturbation. However, the FRF and step responses to surface tilt perturbations do differ from those of the previous robot model (Fig. 5B,C). The lower gain on the ankle joint signal effectively reduces the sensitivity of the control system to surface tilts, thus reducing the magnitude of the FRF gain curve across all frequencies. The phase curves are identical for the previous and improved robot models. The surface tilt step responses are improved relative to the previous model in that the peak body tilt and the peak COM and COP displacements are reduced by half. The reduction in peak COP displacement is indicative of a reduction in the magnitude of corrective torque generated (Equation 1).

Finally, the improved robot control scheme is stable in a sway-referenced surface condition. Although sway-referencing opens the ankle joint feedback loop, there is still sufficient corrective torque generated from the body tilt feedback loop because the controller's K_P and K_D values were selected to be twice the values used by humans. Overall, the improved robot control scheme is more robust than the robot with only ZMP compensation.

4. Discussion

The simple models discussed in this paper are tools for understanding the mechanisms contributing to stance control. The comparison of a simplified model of human stance control with a robot model employing ZMP compensation revealed similarities even though there is little evidence that robot engineers are aware of research results on human stance control. However, the comparison also revealed differences that highlighted deficiencies in the ZMP compensation scheme by demonstrating situations were the robot model becomes unstable while the human model does not. In the spirit of biomimetics, the comparison also led to the suggested addition of a vestibular-like feedback loop to improve the robot stance control system (Fig. 5).

The success of our simple biomimetic exercise suggests that it could be useful to implement more sophisticated control schemes based on current, but still limited knowledge of human stance control mechanisms. Recent experimental work in humans has revealed the presence of very complex stance control schemes that are only partially represented in the simplified human model presented here (Maurer et al., 2006; Schweigart and Mergner, 2008). In fact, some of these more complex mechanisms have been implemented in a humanoid robot (Mergner et al., 2006; Tahboub and Mergner, 2007). This implementation included a sizable feedback time delay as is present in the biological system because a goal of this project was to better understand the human control system. As illustrated in this paper and by others (Masani et al., 2006), a time delay places constraints on the stance control system. But feedback time delay would not necessarily be expected to have an impact on a robot stance control system because the delay could be made arbitrarily small. Therefore, to the extent that a significant biological constraint is removed from the design consideration, one imagines that a robot stance control system could exceed the capabilities of the human system.

Another likely human design constraint is the signal-to-noise properties of sensory systems. Results from studies attempting to understand experimental findings in humans indicate that orientation information from the vestibular sensory system have poorer signal-to-noise properties than proprioceptive and visual sensory systems (van der Kooij et al., 2001). To the extent that humans are able to optimally estimate their orientation by fusing cues from different sensory systems, one expects an overall orientation estimate to be derived from a weighted combination of sensory cues with the weighting factors inversely related to the variability of the sensory signals (Ernst and Banks, 2002).

The effective variability of sensory signals can change in different environmental conditions. Examples include low light conditions were visual orientation signals are degraded, and stance on compliant surfaces where proprioceptive signals are degraded. The combined effects of inherent variability of sensory signals and the need to deal with changing environmental conditions likely have influenced the evolution of the human stance control system. Specifically, the ability of humans to perform sensory re-weighting is a major feature of the human stance control system that compensates for the inherent limitations of sensory systems while performing in complex environments. Sensory re-weighting also adds robustness to the human control system such that loss of sensory function, due to disease, aging, or injury, can be more easily accommodated by the existing re-weighting mechanism without the need for the nervous system to re-learn how to use remaining sensory information.

If robots were expected to perform in complex environments, then we would expect that sensory re-weighting would also be in their control repertoire. However, the implementation may not necessarily be the same as in humans because the design constraints would likely be different. For example, humans have only one set of vestibular receptors that serve multiple purposes. They are used to generate eye movements in the vestibulo-ocular reflex as well as to contribute to postural control during stance and movement. However, the dynamic range of head movements that must be encoded for use in generating vestibulo-ocular reflex eye movements can be 10 to 100 times larger than the range associated with whole body movements. The vestibular receptors must accommodate both functions in humans. But there are more options in a robotic system. One could imagine having multiple vestibular receptors in various locations in the body with different dynamic ranges that are appropriately matched to targeted control functions.

Consideration of how biological systems process vestibular sensory information can facilitate inclusion of artificial vestibular systems in future robot designs. The peripheral vestibular system includes two types of sensors. The semicircular canals sense rotational velocity and otolith organs sense linear acceleration and gravity (Wilson and Jones, 1979). These sensors correspond to manmade rate gyros and linear accelerometers that are available for use in robotic systems. Under dynamic conditions, neither the canals nor the otolith sensors alone are able to provide the vestibular-derived spatial orientation information that was assumed to be available in the human stance control model (Fig. 1B). The justification for the assumption that the vestibular system provides accurate orientation information comes from considerable experimental evidence that, by combining semicircular canal and otolith sensory information, the brain is able to quite accurately estimate head angular velocity, linear acceleration, and tilt with respect to gravity under everyday conditions despite some limitations of the biological sensors (Angelaki et al., 1999). Models that account for the biological processing of canal and otolith information have been developed (MacNeilage et al., 2008; Merfeld and Zupan, 2002; Mergner and Glasauer, 1999; Zupan et al., 2002) and could be used to process rate gyro and linear acceleration signals used in robots. These biologically inspired methods of combining angular rate and linear acceleration signals are surely more robust than the heuristic methods that have been employed in a vestibular-like trunk orientation sensor used in a recent robot design (Löffler et al., 2003).

Humans benefit from an active re-weighting of sensory information used for stance control (Peterka 2002; Mauer et al. 2005). A recent study demonstrated how re-weighting between proprioceptive and vestibular-like sensory orientation information could similarly benefit a robot (Mahboobin et al., 2008). However, this study pre-computed sensory weights that were appropriate for specific test conditions and then manually switched the weights to demonstrate performance improvements. In reality, a robot system would need to automatically control the re-weighting based only upon the array of sensory orientation information available to it. Furthermore, the re-weighting would need to occur in a sufficiently short time interval to prevent loss of balance. The closest realization of such an automatic re-weighting system is in the robot designed by Mergner and colleagues (Mergner et al., 2006; Tahboub and Mergner, 2007) which implements a sensory fusion mechanism that produces robot behavior similar to experimental results in humans (Maurer et al., 2006). As previously mentioned, this robot system was meant to mimic a human system and therefore includes a significant time delay in its feedback control. A robot without time delay and without numerous other biological constraints could potentially benefit from a similar control system, but one imagines that there could be a better design that is more optimally tailored to the specific features and constraints of the robot system.

5. Conclusions

The broad conclusion is that designers of humanoid robots should familiarize themselves with experimental literature in human stance control in order to better appreciate the capabilities of the human system. They should strive to at least match if not exceed human capabilities. If human capabilities are to be exceeded, then it will be important to recognize what mechanisms enhance human function so that these capabilities are included in the robot design. It will also be important to recognize design constraints that differ between humans and robots so that constraints specific to humans do not limit robot design.

Acknowledgments

Supported by NIH grant AG-17960.

7. References

Angelaki DE, McHenry MQ, Dickman JD, Newlands SD, Hess BJ. Computation of inertial motion: Neural strategies to resolve ambiguous otolith information. Journal of Neuroscience 1999;19:316–327. [PubMed: 9870961]

Caballero R, Armada MA, Alarcón P. Methodology for zero-moment point experimental modeling in the frequency domain. Journal of Vibration and Control 2006;12:1385–1406.

Casadio M, Morasso PG, Sanguineti V. Direct measurement of ankle stiffness during quiet standing: implications for control modelling and clinical application. Gait & Posture 2005;21:410–424. [PubMed: 15886131]

Cenciarini M, Peterka RJ. Stimulus-dependent changes in the vestibular contribution to human postural control. J Neurophysiol 2006;95:2733–2750. [PubMed: 16467429]

Collins S, Ruina A, Tedrake R, Wisse M. Efficient bipedal robots based on passive-dynamic walkers. Science 2005;307:1082–1085. [PubMed: 15718465]

Day BL, Severac Cauquil A, Bartolomei L, Pastor MA, Lyon IN. Human body-segment tilts induced by galvanic stimulation: A vestibularly driven balance protection mechanism. J Physiol 1997;500:661–672. [PubMed: 9161984]

Ernst MO, Banks MS. Humans integrate visual and haptic information in a statistically optimal fashion. Nature 2002;415:429–433. [PubMed: 11807554]

Hlavacka F, Njiokiktjien C. Postural responses evoked by sinusoidal galvanic stimulation of the labyrinth. Acta Oto-laryngologica (Stockholm) 1985;99:107–112.

Horak, FB.; Macpherson, JM. Postural Orientation and Equilibrium. In: Rowell, LB.; Shepherd, JT., editors. Handbook of Physiology: Section 12: Exercise: Regulation and Integration of Multiple Systems. Oxford University Press; New York: 1996. p. 255-292.

Kavounoudias A, Gilhodes JC, Roll R, Roll JP. From balance regulation to body orientation: two goals for muscle proprioceptive information processing? Exp Brain Res 1999;124:80–88. [PubMed: 9928792]

Lee DN, Lishman JR. Visual proprioceptive control of stance. Journal of Human Movement Studies 1975;1:87–95.

Löffler K, Gienger M, Pfeiffer F. Sensors and control concept of walking “Johnnie”. International Journal of Robotics Research 2003;22:229–239.

Loram ID, Lakie M. Direct measurement of human ankle stiffness during quiet standing: the intrinsic mechanical stiffness is insufficient for stability. J Physiol 2002;545:1041–1053. [PubMed: 12482906]

MacNeilage PR, Ganesan N, Angelaki DE. Computational approaches to spatial orientation: From transfer functions to dynamic Bayesian inference. Journal of Neurophysiology 2008;100:2981–2996. [PubMed: 18842952]

Magnusson M, Enbom H, Johansson R, Pyykkö I. Significance of pressor input from the human feet in anterior-posterior posture control. Acta Otolaryngol 1990;110:182–188. [PubMed: 2239205]

Mahboobin A, Loughlin PJ, Redfern MS, Anderson SO, Atkeson CG, Hodgins JK. Sensory adaptation in human balance control: Lessons for biomimetic robot bipeds. Neural Networks 2008;21:621–627. [PubMed: 18555957]

Masani K, Vette AH, Popovic MR. Controlling balance during quiet stance: proportional and derivative controller generates preceding motor command to body sway position observed in experiments. Gait & Posture 2006;23:164–172. [PubMed: 16399512]

Maurer C, Mergner T, Bolha B, Hlavacka F. Human balance control during cutaneous stimulation of the plantar soles. Neurosci Lett 2001;302:45–48. [PubMed: 11278108]

Maurer C, Mergner T, Peterka RJ. Multisensory control of human upright stance. Experimental Brain Research 2006;171:231–250.

Merfeld DM, Zupan LH. Neural Processing of Gravitoinertial Cues in Humans. III. Modeling Tilt and Translation Responses. J Neurophysiol 2002;87:819–833. [PubMed: 11826049]

Mergner, T. Modeling sensorimotor control of human upright stance. In: Cisek, P.; Drew, T.; Kalaska, JF., editors. Progress in Brain Research. Elsevier; 2007. p. 283-297.

Mergner T, Glasauer S. A simple model of vestibular canal-otolith signal fusion. Ann NY Acad Sci 1999;871:430–434. [PubMed: 10372098]

Mergner, T.; Huethe, F.; Maurer, C.; Ament, C. In: Zielinska, T.; Zielinska, C., editors. Human equilibrium control principles implemented into a biped robot; Robot Design, Dynamics, and Control (Romansy 16, Sixteenth CISM-IFToMM Symposium); 2006; p. 271-279.

Morasso PG, Sanguineti V. Ankle muscle stiffness alone cannot stabilize balance during quiet standing. Journal of Neurophysiology 2002;88:2157–2162. [PubMed: 12364538]

Nashner LM. Adaptation of human movement to altered environments. Trends in Neurosciences 1982;5:358–361.

Nashner LM, Berthoz A. Visual contribution to rapid motor responses during posture control. Brain Research 1978;150:403–407. [PubMed: 678978]

Nashner LM, Black FO, Wall C III. Adaptation to altered support and visual conditions during stance: Patients with vestibular deficits. Journal of Neuroscience 1982;2:536–544. [PubMed: 6978930]

Peterka RJ. Sensorimotor integration in human postural control. J Neurophysiol 2002;88:1097–1118. [PubMed: 12205132]

Peterka RJ. Simplifying the complexities of maintaining balance. IEEE Eng Med Biol Mag 2003;22:63–68. [PubMed: 12733461]

Peterka RJ, Loughlin PJ. Dynamic regulation of sensorimotor integration in human postural control. J Neurophysiol 2004;91:410–423. [PubMed: 13679407]

Prahlad V, Dip G, Meng-Hwee C. Disturbance rejection by online ZMP compensation. Robotica 2008;26:9–17.

Schweigart G, Mergner T. Human stance control beyond steady state reponse and inverted pendulum simplification. Exp Brain Res 2008;185:635–653. [PubMed: 18030458]

Tahboub K, Mergner T. Biological and engineering approaches to human postural control. Integrated Computer-Aided Engineering 2007;14:15–31.

van der Kooij H, Jacobs R, Koopman B, van der Helm F. An adaptive model of sensory integration in a dynamic environment applied to human stance control. Biol Cybern 2001;84:103–115. [PubMed: 11205347]

van der Kooij H, van Asseldonk E, van Der Helm FCT. Comparison of different methods to identify and quantify balance control. Journal of Neuroscience Methods 2005;145:175–203. [PubMed: 15922036]

Vukobratovic M, Borovac B. Zero moment point - thirty five years of its life. International Journal of Humanoid Robotics 2004;1:157–173.

Wilson, VJ.; Jones, GM. Mammalian Vestibular Physiology. Plenum Press; New York: 1979.

Winter DA, Patla AE, Prince F, Ishac M, Gielo-Perczak K. Stiffness control of balance in quiet standing. J Neurophysiol 1998;80:1211–1221. [PubMed: 9744933]

Zupan LH, Merfeld DM, Darlot C. Using sensory weighting to model the influence of canal, otolith and visual cues on spatial orientation and eye movements. Biol Cybern 2002;86:209–230. [PubMed: 12068787]

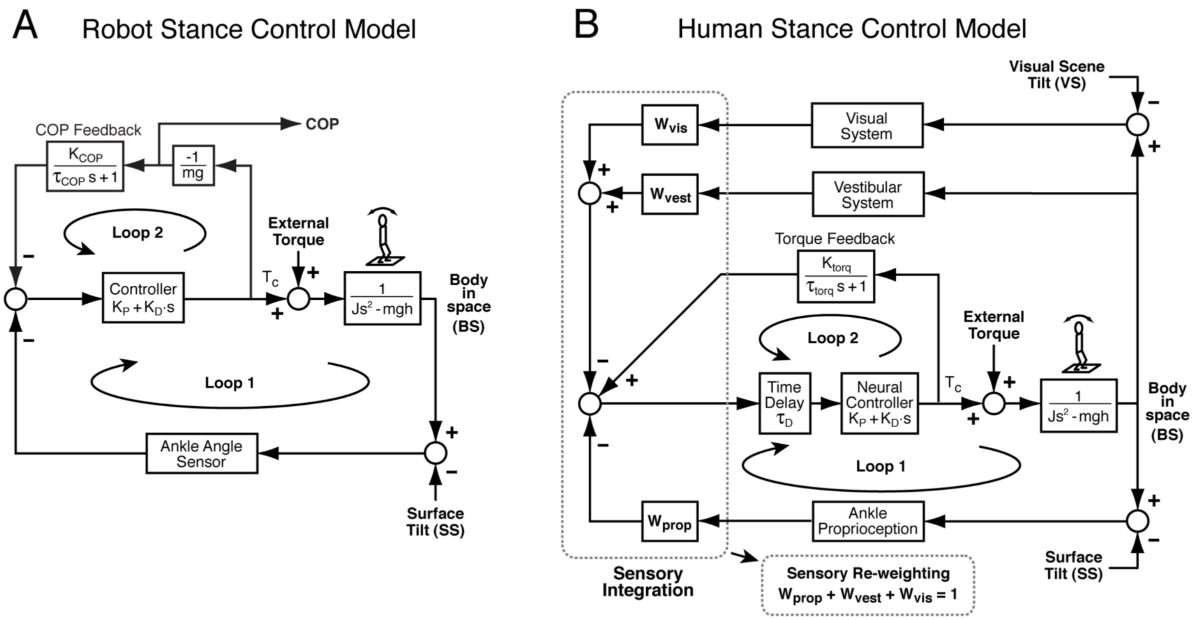

Fig. 1.
Block diagram model of robot stance control using ZMP compensation and a simplified model of human stance control.

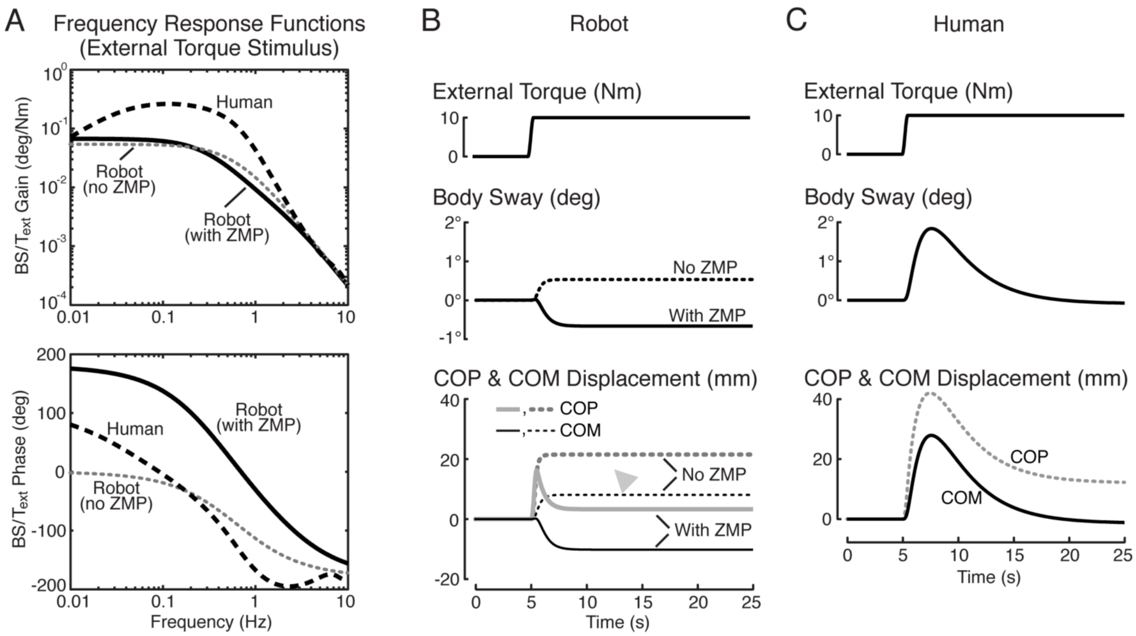

Fig. 2.
Robot and human frequency response functions characterizing body sway responses to external torque perturbations and example time domain responses to a 10 Nm step change in external torque.

NIH-PA Author Manuscript
NIH-PA Author Manuscript

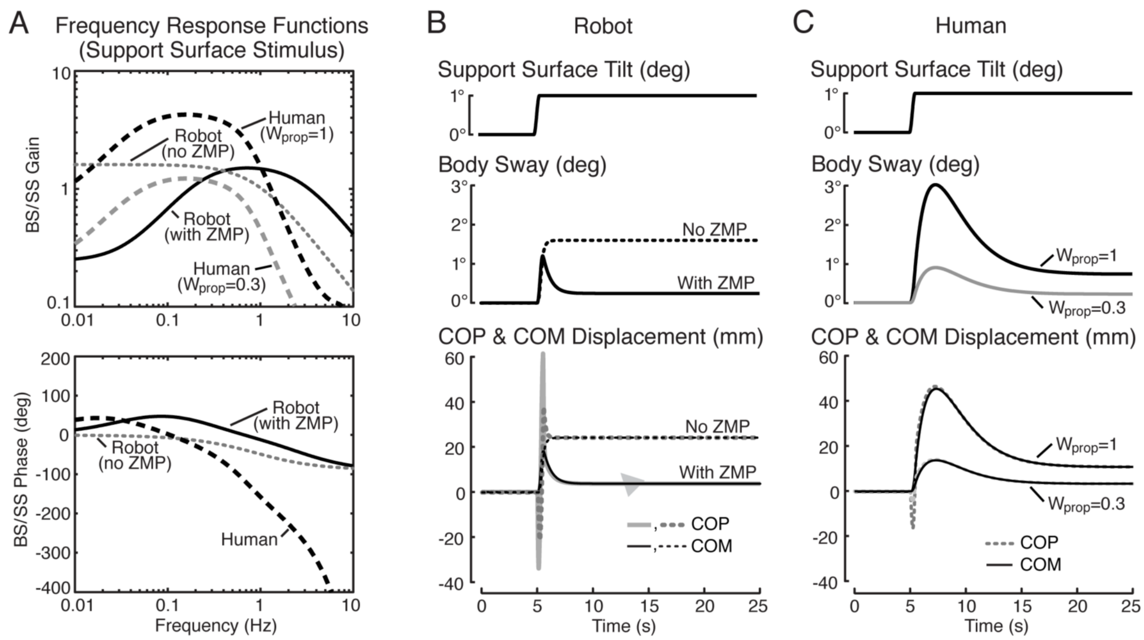

Fig. 3.
Robot and human frequency response functions characterizing body sway responses to support surface tilt perturbations and example time domain responses to a 1° step change in surface tilt.

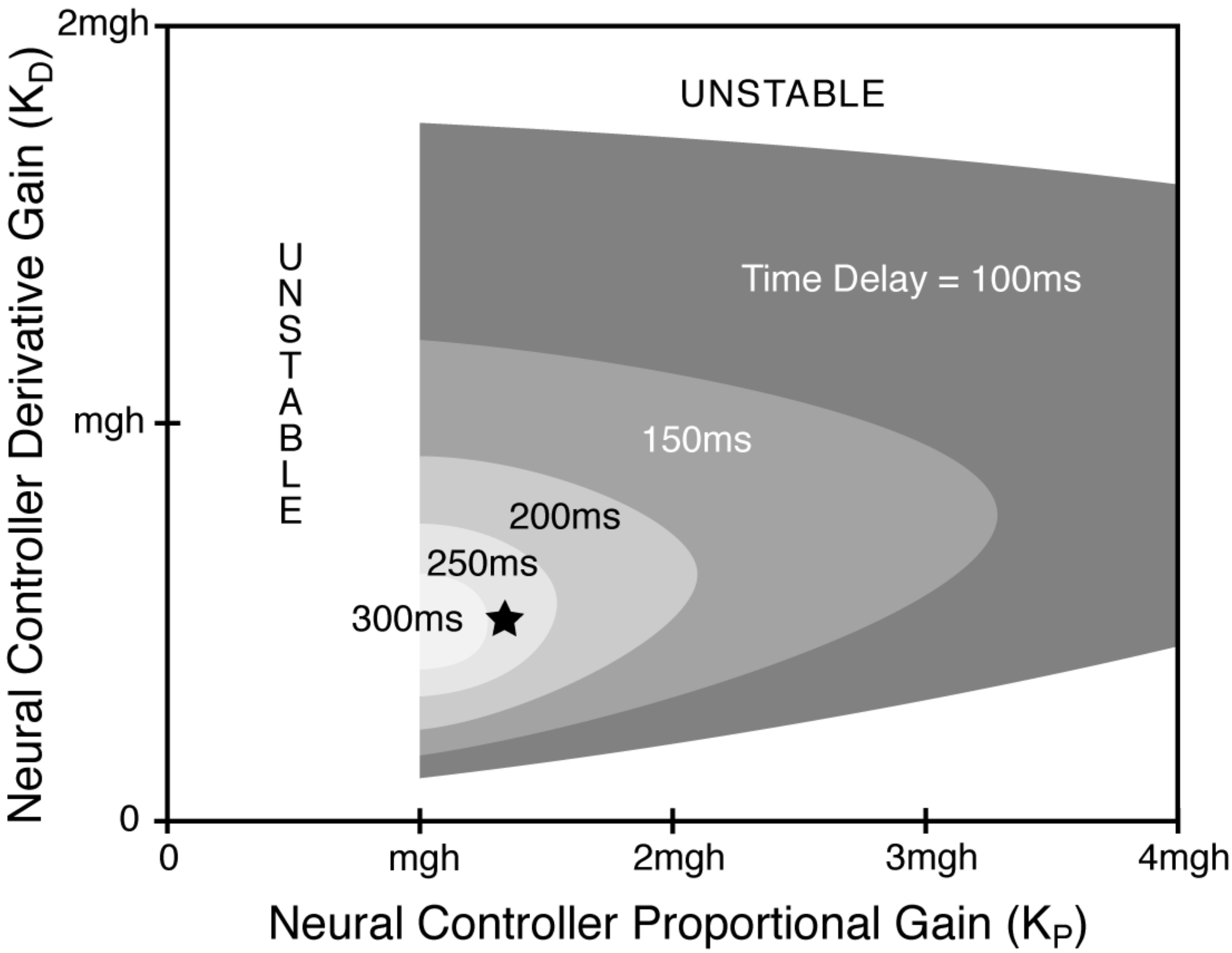

Fig. 4.

Constraints on stance control due to feedback time delay. Region of stable control for different choices of neural controller parameters K_P and K_D are shown for feedback time delays ranging from 100 ms to 300 ms. Experimentally determined (Peterka, 2002) values of K_P and K_D in humans are shown (star).

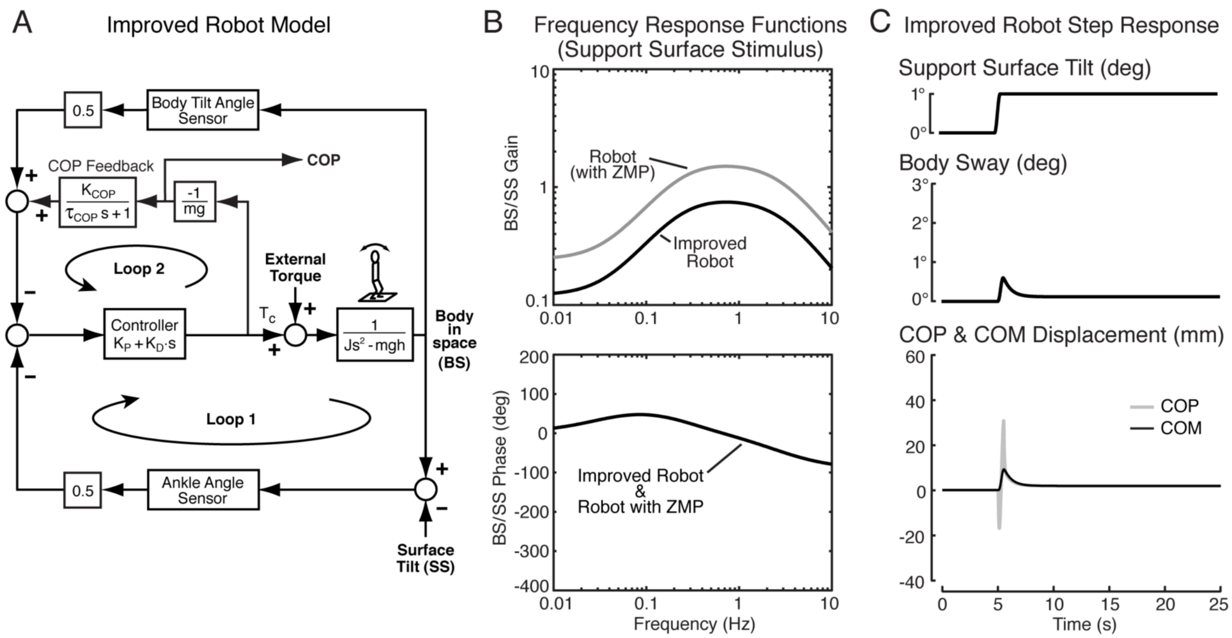

Fig. 5.

Improved robot control model with frequency response functions for support surface perturbations and step responses to 1° surface tilts. Scales on all plots are identical to those used in Fig. 3 to facilitate comparisons.

Table 1

Parameter values used in model simulations

Model Parameter	Units	Human Model	Robot Model	Improved Robot Model
J	kg m^2	66	66	66
m	kg	76	76	76
h	m	0.87	0.87	0.87
K_P	Nm/rad	862	1725	1725
K_D	Nms/rad	302	604	604
τ_D	s	0.15	0	0
K_{torq}	rad/Nm	0.0017	-	-
τ_{torq}	s	20	-	-
K_{COP}	rad/m	-	4	4
τ_{COP}	s	-	4.5	4.5
W_{prop}	-	range 0-1	-	0.5
W_{vest}	-	range 0-1	-	0.5
W_{vis}	-	range 0-1	-	-